Heart Failure after Transcatheter Aortic Valve Implantation: Application of the Most Impactful Strain Imaging Techniques

Gordon M. Burke, MD, Jeffrey J. Popma, MD, and James D. Chang, MD, *West Roxbury and Boston, Massachusetts*

INTRODUCTION

The volume of transcatheter aortic valve implantations (TAVIs) now exceeds the volume of isolated surgical aortic valve replacements (SAVRs) in the United States.[1] The increase in TAVI volume has been attributed to several factors including decreasing mortality rates associated with TAVI and expanding indications for TAVI among lower-risk patients.[1] However, certain procedure-related complication rates are higher among TAVI compared with SAVR including TAVI-induced left bundle branch block (T-LBBB) and right ventricular paced rhythm.[2] Reported rates of new-onset T-LBBB vary from 19% to 55%, and rates of new right ventricular paced rhythm requirement vary from 2% to 51%.[2] Currently, there is a lack of evidence to guide clinical management of these complications.[2] We demonstrate how current speckle-tracking strain imaging techniques can determine the etiology of post-TAVI complications and identify patients most likely to benefit from cardiac resynchronization therapy (CRT).

CASE PRESENTATION

A 91-year-old man with severe aortic stenosis, moderate-to-severe mitral regurgitation, heart failure with reduced ejection fraction, and atrial fibrillation was undergoing workup for elective TAVI after experiencing mild dyspnea on exertion. While waiting for elective TAVI, the patient experienced an acute progression of dyspnea and lower extremity edema. The patient subsequently presented to the emergency room and was admitted for acute heart failure decompensation. The etiology of the patient's heart failure decompensation was believed to be primarily driven by progression of the severe aortic stenosis. During this admission, the patient underwent TAVI complicated by new-onset T-LBBB. Within 1 month following discharge, the patient required 2 additional hospitalizations for heart failure.

From the VA Boston Healthcare System, Cardiology Section 111CA, West Roxbury (G.M.B.); Harvard Medical School (G.M.B., J.J.P., J.D.C.); and Division of Cardiovascular Medicine, Beth Israel Deaconess Medical Center, Boston, Massachusetts (J.J.P., J.D.C.).

Keywords: Speckle-tracking echocardiography, Transcatheter aortic valve implantation, Cardiac resynchronization therapy, Strain rate imaging

Correspondence: Gordon M. Burke, MD, VA Boston Healthcare System, Cardiology Section 111CA, 1400 VFW Parkway, West Roxbury, MA 02132. (E-mail: *Gordon.Burke@va.gov*).

2468-6441
https://doi.org/10.1016/j.case.2023.10.003

VIDEO HIGHLIGHTS

Video 1: Pre-TAVI 2D TTE apical 4-chamber view demonstrating underlying atrial fibrillation, increased left ventricular end-diastolic dimension (5.9 cm), moderately reduced LVEF (38%), mildly reduced right ventricular systolic function, and severe biatrial enlargement.

Video 2: Pre-TAVI 2D TTE apical 4-chamber view longitudinal strain analysis with segmental strain values and corresponding strain curves. The absolute strain values in this view are severely reduced with an average longitudinal strain of −9.0. The strain curves demonstrate synchronous deformation with similar TPLS among all segments.

Video 3: Post-TAVI 2D TTE apical 5-chamber view with color Doppler demonstrating mild paravalvular leak of the aortic valve bioprosthesis with some visualization of moderate-to-severe mitral regurgitation and mild-to-moderate tricuspid regurgitation.

Video 4: Post-TAVI 2D TTE apical 4-chamber view after developing a T-LBBB demonstrating septal flash, apical rocking, underlying atrial fibrillation, top-normal left ventricular end diastolic dimension (5.7 cm), severely reduced LVEF (25%), moderately reduced right ventricular systolic function, and severe biatrial enlargement.

Video 5: Post-TAVI 2D TTE apical 4-chamber view longitudinal strain analysis with segmental strain values and corresponding strain curves. The absolute strain values in this view are very severely reduced with an average longitudinal strain of −6.7. The strain curves demonstrate the classic LBBB pattern.

Video 6: Post-CRT 2D TTE apical 4-chamber view demonstrating underlying atrial fibrillation with biventricular pacing, normal left ventricular end-diastolic dimension (5.3 cm), moderately reduced LVEF (36%), mildly reduced right ventricular systolic function, and severe biatrial enlargement.

Video 7: Post-CRT 2D TTE apical 4-chamber view longitudinal strain analysis with segmental strain values and corresponding strain curves. The absolute strain values in this view are severely reduced with an average longitudinal strain of −10.3. The strain curves demonstrate very synchronous deformation with mostly overlapping strain curves and very similar TPLS among all segments.

View the video content online at www.cvcasejournal.com.

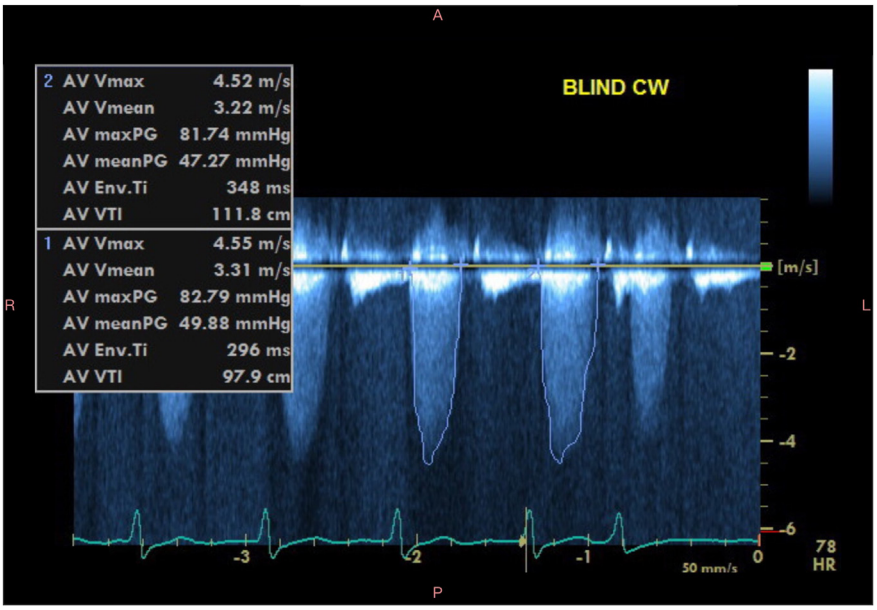

Figure 1 Pre-TAVI TTE apical 5-chamber continuous-wave (CW) Doppler across the aortic valve demonstrating severe stenosis with a peak aortic velocity of 4.6 m/sec, peak gradient of 83 mm Hg, and mean gradient of 50 mm Hg.

Table 1 Pre-TAVI, Post-TAVI, and post-CRT 2D TTE and ECG findings

	Pre-TAVI	Post-TAVI	Post-CRT
Aortic valve			
Peak velocity, m/sec	4.6	1.2	1.3
Peak gradient, mm Hg	83	6	7
Left ventricular end-diastolic dimension, cm	5.9	5.7	5.3
LVEF, %	38	25	36
GLS, %	–9.1	–7.1	–9.6
MD, msec	51	101	36
Mitral regurgitation	Severe	Moderate-severe	Moderate
Effective regurgitant orifice, cm^2	0.39	0.33	0.27
Regurgitant volume, mL	59	52	42
Tricuspid regurgitation	Mild-moderate	Mild-moderate	Mild-moderate
Right ventricular systolic pressure, mm Hg	34	36	26
Right ventricular systolic function	Mildly reduced	Moderately reduced	Mildly reduced
Tricuspid annular plane systolic excursion, cm	1.4	1.2	1.5
Biatrial size	Severely enlarged	Severely enlarged	Severely enlarged
QRS duration, msec	106	148	144

The patient was regularly followed as an outpatient prior to undergoing TAVI. The patient's cardiac medications included aspirin, atorvastatin, furosemide, lisinopril, metoprolol, spironolactone, and warfarin. The patient's pre-TAVI transthoracic echocardiogram (TTE) demonstrated severe aortic stenosis (peak velocity, 4.6 m/sec; peak gradient, 83 mm Hg; Figure 1), mild left ventricular cavity dilation (end-diastolic dimension, 5.9 cm), moderate global left ventricular systolic dysfunction with a left ventricular ejection fraction (LVEF) of 38% (Video 1), severe mitral regurgitation, mild-to-moderate tricuspid regurgitation, estimated right ventricular systolic pressure of 34 mm Hg, mildly reduced right ventricular systolic function, and severe biatrial enlargement (Table 1). The patient's pre-TAVI electrocardiogram (ECG) was notable for atrial fibrillation, intermediate QRS duration of 106 msec, and nonspecific ST changes (Figure 2A). The etiology of the patient's mitral regurgitation was a result of left ventricular dilation from multivalvular disease and annular dilation from long-standing atrial fibrillation. Strain assessment of the pre-TAVI TTE demonstrated a global longitudinal strain (GLS) of −9.1 and a mechanical dispersion (MD), calculated as the SD of the time to peak longitudinal strain (TPLS) values, of 51 msec (Table 1, Video 2, Figure 2B, C, and D).

The patient had undergone a nuclear pyrophosphate scan as part of the pre-TAVI evaluation that showed no evidence of transthyretin

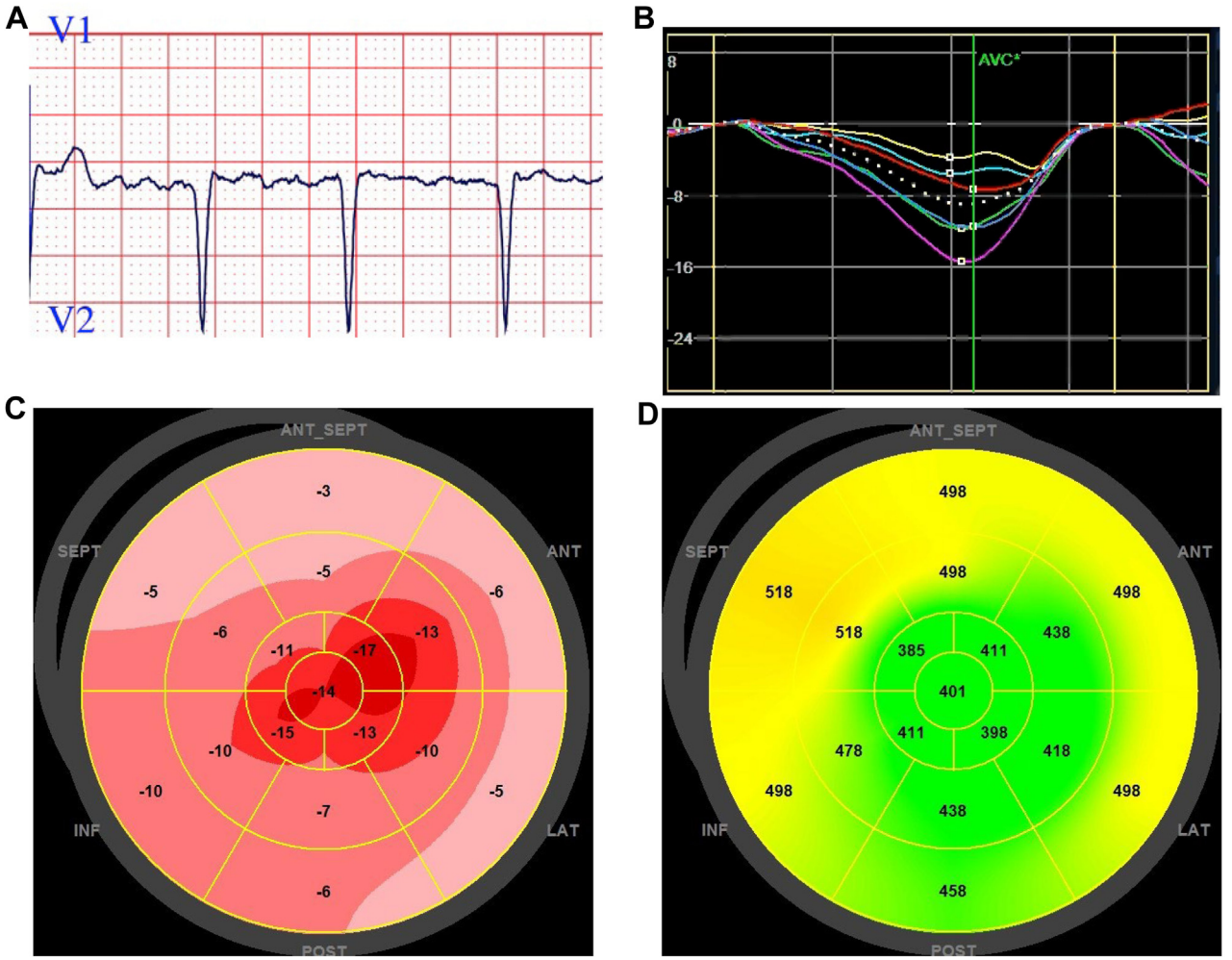

Figure 2 **(A)** Pre-TAVI ECG is notable for underlying atrial fibrillation and an intermediate QRS duration of 106 msec. **(B)** Two-dimensional TTE apical 4-chamber view segmental strain curves. **(C)** Global longitudinal strain polar map with a GLS of –9.1 consistent with severely reduced systolic function. **(D)** Time to peak longitudinal strain polar map with an MD of 51 msec. The strain curves **(B)**, TPLS polar map **(D)**, and low MD demonstrate synchronous systolic function consistent with an absence of focal myocardial scar from ischemia.

cardiac amyloidosis. The patient received a 29 mm self-expanding valve. There was mild paravalvular leak visualized during the intraprocedural transesophageal echocardiogram and on post-TAVI TTE (Video 3). The post-TAVI TTE demonstrated normal transvalvular gradients across the aortic valve bioprosthesis (peak velocity, 1.2 m/sec; peak gradient, 6 mm Hg; Figure 3). The patient denied any chest pain following the procedure, and subsequent hospitalizations did not meet conventional criteria for an acute coronary syndrome.

Following discharge from the TAVI hospitalization, the patient was readmitted 3 days later for heart failure. The patient received intravenous diuretics and was later discharged on a higher dose of oral diuretic. However, the patient's heart failure symptoms returned, and the patient required hospitalization again 4 days later.

After developing a T-LBBB, the ECG was notable for a QRS duration of 148 msec (Figure 4A), and the TTE demonstrated a decline in left ventricular systolic function with an LVEF of 25%, GLS of −7.1, and MD of 101 msec (Table 1, Videos 4 and 5, Figure 4B, C, and D). The segmental strain curves, GLS polar map, and TPLS polar map (Figure 4B, C, and D) demonstrate the decline in myocardial deformation and dyssynchronous activation sequence caused by the T-LBBB consistent with the markedly elevated MD. Also, the patient's post-TAVI TTE demonstrated a slight decrease in left ventricular cavity size (end-diastolic dimension, 5.7 cm), right ventricular systolic function (moderately reduced), and mitral regurgitation (moderate-to-severe) with continued mild-to-moderate tricuspid regurgitation and estimated right ventricular systolic pressure of 36 mm Hg (Table 1).

Despite intensification of the patient's cardiac medications, the patient required a second hospitalization within 1 month post-TAVI for recurrent heart failure. During this hospitalization, the patient was evaluated for possible invasive therapies and underwent CRT implantation prior to discharge. Following CRT implantation, the patient's ECG demonstrated a QRS duration of 144 msec (Figure 5A), and the patient's TTE showed an improvement in systolic function with an LVEF of 36%, GLS of −9.6, and MD of 36 msec (Videos 6 and 7, Figure 5B, C, and D). The segmental strain curves and TPLS polar map (Figure 5B and D) demonstrate the homogeneous activation sequence of the left ventricle post-CRT and the resultant reduction in MD. The patient's post-CRT TTE also demonstrated further

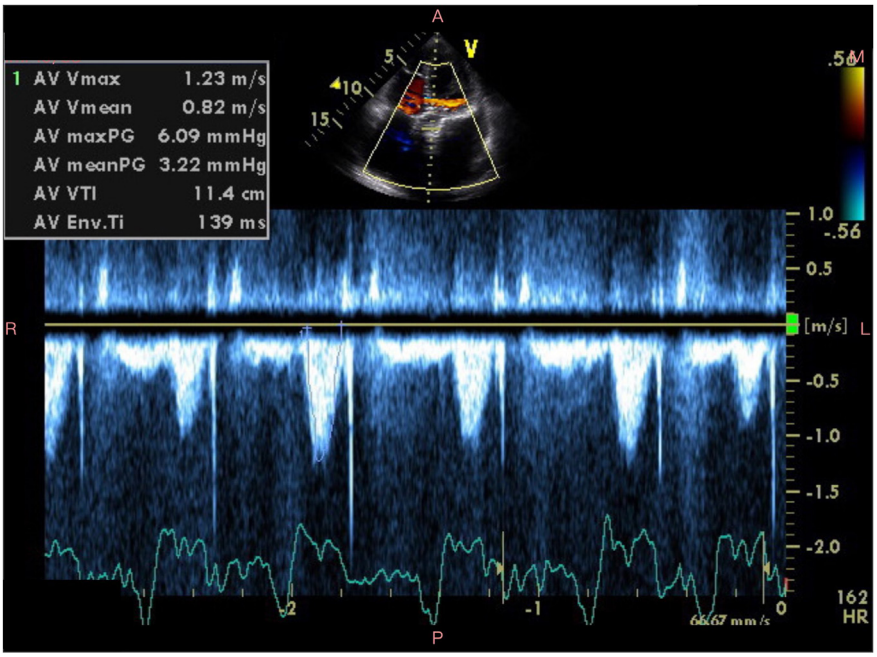

Figure 3 Post-TAVI TTE apical 5-chamber continuous-wave Doppler across the aortic valve bioprosthesis demonstrating normal hemodynamic profile with peak aortic velocity of 1.2 m/sec, peak gradient of 6 mm Hg, and mean gradient of 3 mm Hg.

decrease in left ventricular cavity size (end-diastolic dimension 5.3 cm), mitral regurgitation (moderate), and estimated right ventricular systolic pressure (26 mm Hg) with improved right ventricular systolic function (mildly reduced) and continued mild-to-moderate tricuspid regurgitation (Table 1).

DISCUSSION

Patients with left bundle branch block (LBBB) are often considered a single cohort of patients. However, the underlying pathophysiology and resultant left ventricular activation sequence among patients with LBBB varies widely and, as a result, poses challenges when trying to provide generalized recommendations regarding the evaluation and treatment of this patient population. Although heterogenous based upon underlying left ventricular pathology, evidence from endocardial catheter mapping among patients with LBBB has demonstrated that the initial site of left ventricular activation generally occurs at or adjacent to the septum, and the latest site of left ventricular activation generally occurs at or adjacent to the lateral segments, with more variability among patients with a history of coronary artery disease.[3] In addition, endocardial catheter mapping data have demonstrated that patients with a history of coronary artery disease have the longest left ventricular activation sequence and longest QRS duration.[3]

Transcatheter aortic valve implantation–induced LBBB is a relatively common complication of TAVI, occurring in 19% to 55% of patients.[2] The clinical implications of T-LBBBs are unclear as some studies have demonstrated higher rates of mortality, while others have shown no increase in rates of hospitalization or mortality.[2] Current clinical guidelines in the United States highlight the lack of available data to support surveillance and management of T-LBBBs and state "further investigation in this area is needed."[2]

The discrepancies in reported outcomes among patients with T-LBBB are likely due to a combination of factors including the heterogeneity of baseline clinical characteristics, mechanisms of T-LBBB, and definitions of T-LBBB. Pre-TAVI clinical characteristics associated with increased risk of T-LBBB include prolonged QRS duration and prior coronary artery bypass graft surgery.[4] Several mechanisms during the TAVI procedure can contribute to a T-LBBB, which most frequently occurs during expansion of the bioprosthesis (especially during overexpansion) but may occur while passing the guidewire into the left ventricle and during balloon predilation.[4] Valve type, model, and size as well as procedural techniques also impact the likelihood for T-LBBB.[4] When T-LBBB was defined as present on ECG at discharge or 7 days post-TAVI, these patients had a higher rate of permanent pacemaker implantation and lack of LVEF improvement but no difference in cardiovascular mortality or heart failure hospitalization compared with those without T-LBBB at 12-month follow-up.[5] However, new-onset T-LBBB resolves among 36.6% to 42.2% of patients at 1 year.[5,6] Patients with a persistent T-LBBB at 1-year follow-up demonstrated an increase in mortality compared with those with no LBBB or a temporary LBBB.[6]

In general, strain imaging patterns should reflect left ventricular function, which is often reduced among patients with severe symptomatic aortic stenosis.[7] Investigators have postulated that certain imaging techniques, such as strain imaging, may detect earlier, reversible stages of diffuse fibrosis of the left ventricle prior to symptom onset and may assist in optimizing timing of TAVI.[7]

In addition to GLS, there are regional longitudinal strain patterns commonly found among patients with aortic stenosis. There is often a mild gradient of increasing absolute values of longitudinal strain from base to apex.[8] This increasing gradient of absolute longitudinal strain values from base to apex is often associated with the "apical sparing" pattern seen in cardiac amyloidosis, but it can be seen in other disease states involving left ventricular hypertrophy including aortic

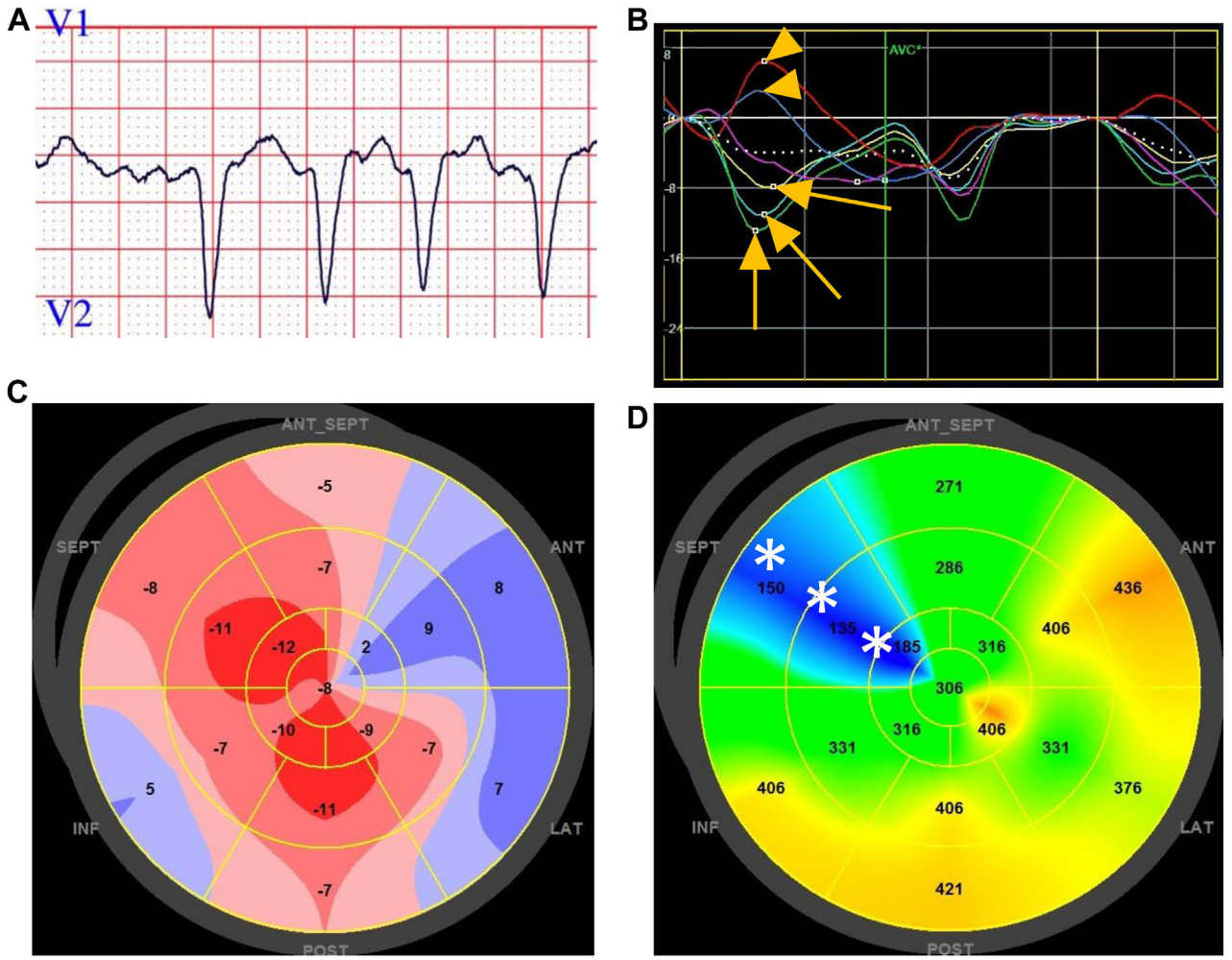

Figure 4 **(A)** Post-TAVI ECG is notable for underlying atrial fibrillation and T-LBBB with a prolonged QRS duration of 148 msec. **(B)** Two-dimensional TTE apical 4-chamber view segmental strain curves. **(C)** Global longitudinal strain polar map with a GLS of –7.1 consistent with very severely reduced systolic function. **(D)** Time to peak longitudinal strain polar map with a significantly increased MD of 101 msec. Segmental strain curves **(B)** demonstrate early peak contraction (*arrows*) followed by rebound stretch and delayed second contraction of the septal segments and early stretching (*arrowheads*) with delayed peak contraction of the lateral segments consistent with the classic LBBB pattern. *Asterisks* **(D)** and *arrows* **(B)** indicate early septal activation consistent with septal flash seen in the classic LBBB pattern.

stenosis and hypertrophic cardiomyopathy.[8] Using a cutoff value of at least 1.0 for relative apical longitudinal strain, defined as the average apical longitudinal strain divided by the sum of the average mid longitudinal strain and average basal longitudinal strain, can differentiate cardiac amyloidosis from other causes of left ventricular hypertrophy.[8] The pre-TAVI relative apical longitudinal strain in our patient was 0.94, consistent with the absence of cardiac amyloidosis.

There are several different imaging methods that have been validated among patients with LBBB as predictors regarding clinical response to CRT. This can be demonstrated using a variety of imaging techniques that confirm the presence of certain interactions among the septal/anteroseptal walls with the lateral/inferolateral walls as these are, respectively, the sites of earliest and latest left ventricular activation in LBBB in the absence of coronary disease.[3] The presence of nonviable myocardium, particularly scar from ischemia, is associated with a poor response to CRT.[9]

One method to evaluate for the potential response to CRT among patients with LBBB includes qualitative visual assessments of two-dimensional (2D) TTE videos to determine the presence of septal flash and apical rocking.[10] Septal flash refers to the rapid motion of the septum toward the center of the left ventricular cavity, and apical rocking refers to early motion of the apical septum transitioning to slower motion of the lateral segments.[10] However, subsequent studies have demonstrated considerable variability regarding assessment of septal flash and apical rocking, suggesting challenges in the generalizability of these visual characteristics.[9]

Strain imaging has identified different LBBB patterns of left ventricular activation and their associated responses to CRT. The description of a "classic" LBBB pattern using strain imaging involves early peak contraction of the basal septal wall, representing septal flash, occurring simultaneously with early stretch of the basal lateral wall.[11,12] The

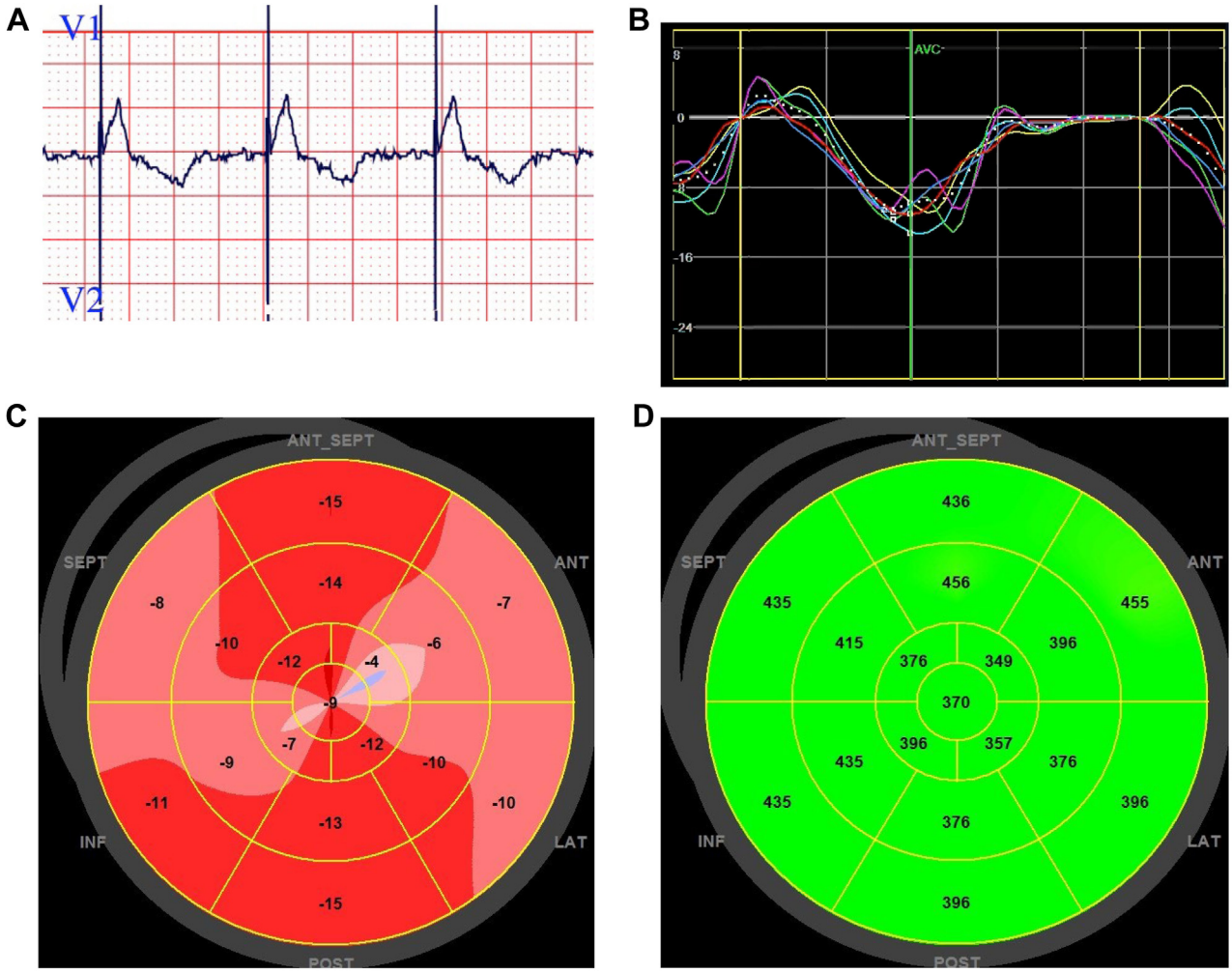

Figure 5 **(A)** Post-CRT ECG is notable for underlying atrial fibrillation and biventricular pacing with a QRS duration of 144 msec. **(B)** Two-dimensional TTE apical 4-chamber view segmental strain curves. **(C)** Global longitudinal strain polar map with a GLS of –9.6 consistent with severely reduced systolic function. **(D)** Time to peak longitudinal strain polar map with an MD of 36 msec. The strain curves **(B)**, TPLS polar map **(D)**, and low MD demonstrate a highly synchronous activation sequence of the left ventricle indicative of a favorable response to CRT.

septal wall then demonstrates rebound stretch during lateral wall contraction. The lateral wall demonstrates delayed peak contraction occurring after aortic valve closure. The septal wall demonstrates a second, smaller contraction around the time of or after aortic valve closure.[11,12] This classic LBBB pattern is associated with a favorable response to CRT.[11] Our patient displayed septal flash, apical rocking, and the classic LBBB pattern post-TAVI (Videos 4 and 5; Figure 4B and D). Of note, these imaging findings vary slightly from the classic descriptions in this case on account of the patient's significant cardiac comorbidities including permanent atrial fibrillation and resultant loss of effective atrial contraction, reduced left ventricular systolic function, and significant multivalvular disease.

In addition to the qualitative appearance of the strain curves, certain quantitative strain measures provide important prognostic value. Among patients with moderate or severe left ventricular systolic dysfunction, an MD of ≥75 msec is an independent predictor of ventricular arrhythmias and an MD of <75 msec correlates with lower ventricular arrhythmias irrespective of LVEF.[13] In addition, a significant decrease in MD after CRT implantation correlates with improved clinical outcomes.[14]

Similar techniques associated with a positive clinical response to CRT using cardiac magnetic resonance imaging include demonstrating the presence of septal viability, increased lateral wall work, and decreased septal wall work.[9] These imaging findings are analogous to the early systolic stretch followed by an uninterrupted and dominant contraction of the lateral wall in concert with the less dominant and interrupted contraction of the septal wall demonstrated in the classic LBBB pattern on strain imaging.[11,12]

Six weeks after TAVI, the patient underwent CRT implantation and did not require hospitalization for over 1 year thereafter. Despite a modest improvement in LVEF and decrease in QRS duration post-CRT, evaluation using strain imaging—specifically, in this case, the appearance of the strain curves, appearance of the TPLS polar maps, and the MD values—most accurately characterized the etiology of the patient's clinical decline post-TAVI and significant improvement in clinical status post-CRT. The patient's comorbidities, particularly the

long-standing history of permanent atrial fibrillation, likely contributed to the somewhat atypical appearance of systolic function post-CRT. The patient's systolic function post-CRT lacks an effective atrial load of the left ventricle, resulting in a somewhat abrupt appearance at the onset of systole with a subsequent highly synchronous activation of the left ventricle (Videos 6 and 7).

Certain strain measures may be more clinically relevant depending on a patient's comorbidities, the cardiac pathology of interest, and the available strain vendor used in clinical practice. In our experience, different strain and other imaging assessments may provide more valuable clinical insight on a case-by-case basis. In general, we have found that incorporating changes in strain and other imaging assessments over time often indicates which findings are most germane to a particular clinical question or concern. Consistent with the recommendations from the European Association of Cardiovascular Imaging, American Society of Echocardiography, and industry vendors task force, we recommend emphasizing the appearance of segmental strain curves over segmental strain values given the high intervendor variability.[15]

CONCLUSION

Transcatheter aortic valve implantation is a safe and effective therapy in the treatment of severe aortic stenosis, but it comes with unique complications including higher rates of LBBB. Utilization of strain imaging can improve clinical management of patients with T-LBBBs particularly in terms of providing more insight into which patients would derive the most benefit from CRT implantation. Comparison of strain assessments, particularly the appearance of segmental strain curves, before and after TAVI can better clarify the underlying pathophysiology among patients with a change in clinical status compared with routine imaging assessments, guide subsequent clinical decision-making for providers, and improve clinical outcomes for patients.

CONSENT STATEMENT

The authors declare that since this was a non-interventional, retrospective, observational study utilizing de-identified data, informed consent was not required from the patient under an IRB exemption status.

ETHICS STATEMENT

The authors declare that the work described has been carried out in accordance with The Code of Ethics of the World Medical Association (Declaration of Helsinki) for experiments involving humans.

FUNDING STATEMENT

The authors declare that this report did not receive any specific grant from funding agencies in the public, commercial, or not-for-profit sectors.

DISCLOSURE STATEMENT

J.J.P. is employed by Medtronic (Minneapolis, MN) and receives research grants and personal fees from Edwards Lifesciences (Irvine, CA), grants from Boston Scientific (Marlborough, MA), and grants from Abbott Vascular (Murrieta, CA). G.M.B. and J.D.C. have no declarations of interest.

SUPPLEMENTARY DATA

Supplementary data related to this article can be found at https://doi.org/10.1016/j.case.2023.10.003.

REFERENCES

1. Mori M, Gupta A, Wang Y, Vahl T, Nazif T, Kirtane AJ, et al. Trends in transcatheter and surgical aortic valve replacement among older adults in the United States. J Am Coll Cardiol 2021;78:2161-72.
2. Kusumoto FM, Schoenfeld MH, Barrett C, Edgerton JR, Ellenbogen KA, Gold MR, et al. 2018 ACC/AHA/HRS guideline on the evaluation and management of patients with bradycardia and cardiac conduction delay: executive summary: a report of the American College of Cardiology/American heart association task force on clinical practice guidelines, and the heart rhythm Society. J Am Coll Cardiol 2019;74:932-87.
3. Vassallo JA, Cassidy DM, Marchlinski FE, Buxton AE, Waxman HL, Doherty JU, et al. Endocardial activation of left bundle branch block. Circulation 1984;69:914-23.
4. Auffret V, Puri R, Urena M, Chamandi C, Rodriguez-Gabella T, Philippon F, et al. Conduction disturbances after transcatheter aortic valve replacement: current status and future perspectives. Circulation 2017;136:1049-69.
5. Nazif TM, Williams MR, Hahn RT, Kapadia S, Babaliaros V, Rodes-Cabau J, et al. Clinical implications of new-onset left bundle branch block after transcatheter aortic valve replacement: analysis of the PARTNER experience. Eur Heart J 2014;35:1599-607.
6. Houthuizen P, van der Boon RM, Urena M, Van Mieghem N, Brueren GB, Poels TT, et al. Occurrence, fate and consequences of ventricular conduction abnormalities after transcatheter aortic valve implantation. EuroIntervention 2014;9:1142-50.
7. Vollema EM, Amanullah MR, Prihadi EA, Ng ACT, van der Bijl P, Sin YK, et al. Incremental value of left ventricular global longitudinal strain in a newly proposed staging classification based on cardiac damage in patients with severe aortic stenosis. Eur Heart J Cardiovasc Imaging 2020;21:1248-58.
8. Phelan D, Collier P, Thavendiranathan P, Popovic ZB, Hanna M, Plana JC, et al. Relative apical sparing of longitudinal strain using two-dimensional speckle-tracking echocardiography is both sensitive and specific for the diagnosis of cardiac amyloidosis. Heart 2012;98:1442-8.
9. Aalen JM, Donal E, Larsen CK, Duchenne J, Lederlin M, Cvijic M, et al. Imaging predictors of response to cardiac resynchronization therapy: left ventricular work asymmetry by echocardiography and septal viability by cardiac magnetic resonance. Eur Heart J 2020;41:3813-23.
10. Stankovic I, Prinz C, Ciarka A, Daraban AM, Kotrc M, Aarones M, et al. Relationship of visually assessed apical rocking and septal flash to response and long-term survival following cardiac resynchronization therapy (PREDICT-CRT). Eur Heart J Cardiovasc Imaging 2016;17:262-9.
11. Calle S, Kamoen V, De Buyzere M, De Pooter J, Timmermans F. A strain-based staging classification of left bundle branch block-induced cardiac remodeling. JACC Cardiovasc Imaging 2021;14:1691-702.
12. Klein MR, Sundh F, Simlund J, Harrison JK, Jackson KP, Hughes GC, et al. Immediate mechanical effects of acute left bundle branch block by speckle tracked strain. J Electrocardiol 2015;48:643-51.
13. Perry R, Patil S, Marx C, Horsfall M, Chew DP, Sree Raman K, et al. Advanced echocardiographic imaging for prediction of SCD in moderate and severe LV systolic function. JACC Cardiovasc Imaging 2020;13:604-12.
14. Hasselberg NE, Haugaa KH, Bernard A, Ribe MP, Kongsgaard E, Donal E, et al. Left ventricular markers of mortality and ventricular arrhythmias in heart failure patients with cardiac resynchronization therapy. Eur Heart J Cardiovasc Imaging 2016;17:343-50.
15. Mirea O, Pagourelias ED, Duchenne J, Bogaert J, Thomas JD, Badano LP, et al. Variability and reproducibility of segmental longitudinal strain measurement: a report from the EACVI-ASE strain standardization task force. JACC Cardiovasc Imaging 2018;11:15-24.